White Rose Research Online

eprints@whiterose.ac.uk
https://eprints.whiterose.ac.uk
Universities of Leeds, Sheffield and York

Deposited via The University of Sheffield.

White Rose Research Online URL for this paper:
https://eprints.whiterose.ac.uk/id/eprint/127228/

Version: Accepted Version

Article:
Carretta, Y., Hunter, A., Boman, R. et al. (2018) Ultrasonic roll bite measurements in cold rolling: Contact length and strip thickness. Proceedings of the Institution of Mechanical Engineers, Part J: Journal of Engineering Tribology, 232 (2). pp. 179-192. ISSN: 1350-6501

https://doi.org/10.1177/1350650117712314

Carretta Y, Hunter A, Boman R, et al. Ultrasonic roll bite measurements in cold rolling: Contact length and strip thickness. Proceedings of the Institution of Mechanical Engineers, Part J: Journal of Engineering Tribology. 2018;232(2):179-192. Copyright © IMechE 2017. DOI: https://doi.org/10.1177/1350650117712314. Article available under the terms of the CC-BY-NC-ND licence (https://creativecommons.org/licenses/by-nc-nd/4.0/).

Reuse
This article is distributed under the terms of the Creative Commons Attribution-NonCommercial-NoDerivs (CC BY-NC-ND) licence. This licence only allows you to download this work and share it with others as long as you credit the authors, but you can't change the article in any way or use it commercially. More information and the full terms of the licence here: https://creativecommons.org/licenses/

Takedown
If you consider content in White Rose Research Online to be in breach of UK law, please notify us by emailing eprints@whiterose.ac.uk including the URL of the record and the reason for the withdrawal request.

UNIVERSITY OF LEEDS
University of Sheffield
UNIVERSITY of York

Ultrasonic roll bite measurements in cold rolling - contact length and strip thickness

Y Carretta[1], A Hunter[2],

R Boman[1], J-P Ponthot[1],

N Legrand[3], M Laugier[3]

R Dwyer-Joyce[2]

[1] Department of Aerospace and Mechanical Engineering, University of Liège, Belgium

yvescarretta@gmail.com

r.boman@ulg.ac.be

jp.ponthot@ulg.ac.be

[2] The Leonardo Centre for Tribology, Department of Mechanical Engineering, University of Sheffield, Sheffield, UK

a.k.hunter@sheffield.ac.uk

r.dwyerjoyce@sheffield.ac.uk*

[3]ArcelorMittal Global R&D, Maizières-les-Metz, France

nicolas.legrand@arcelormittal.com

maxime.laugier@arcelormittal.com

* corresponding author

Ultrasonic measurements in cold rolling: contact length and strip thickness

Abstract.

In cold rolling of thin metal strip, contact conditions between the work rolls and the strip are of great importance: roll deformations and their effect on strip thickness variation may lead to strip flatness defects and thickness inhomogeneity. To control the process, online process measurements are usually carried out; such as the rolling load, forward slip and strip tensions at each stand. Shape defects of the strip are usually evaluated after the last stand of a rolling mill thanks to a flatness measuring roll. However, none of these measurements is made within the roll bite itself due to the harsh conditions taking place in that area.

This paper presents a sensor capable of monitoring strip thickness variations as well as roll bite length in situ and in real time. The sensor emits ultrasonic pulses that reflect from the interface between the roll and the strip. Both the time-of-flight (ToF) of the pulses and the reflection coefficient (the ratio of the amplitude of the reflected signal to that of the incident signal) are recorded.

The sensor system was incorporated into a work roll and tested on a pilot rolling mill. Measurements were taken as steel strips were rolled under several lubrication conditions. Strip thickness variation and roll-bite length obtained from the experimental data agree well with numerical results computed with a cold rolling model in the mixed lubrication regime.

Keywords.

Ultrasound, Cold Rolling, Roll Bite, Strip Thickness, Roll-Bite Length, Numerical Modelling.

Nomenclature

R	reflection coefficient
z	acoustic impedance, MRayls
t	time of flight, s
c	speed of sound, m/s
d_0	initial ultrasonic path length, mm
α	acoustoelastic constant
λ	wavelength of the ultrasonic pulse, mm
ω	angular frequency of the wave, rad/s
K	interface stiffness, GPa/µm
$\bar{\varepsilon}^p$	equivalent plastic strain, -
σ_y	yield limit, MPa
k	yield shear stress, MPa
E	Young's modulus, MPa
ν	Poisson's ratio, -
η	lubricant dynamic viscosity, MPa.s
η_g	lubricant dynamic viscosity when $T = T_g$
p_l	lubricant pressure, MPa
T	temperature, K
T_g	glass transition temperature, K
A_1, A_2	
B_1, B_2	Williams-Landel-Ferry equation constants
C_1, C_2	
R_a	arithmetic roughness, µm
R_q	composite roughness, µm
$R_{q,strip}$	quadratic roughness of the strip, µm
$R_{q,rolls}$	quadratic roughness of the rolls, µm
ll	half distance between asperities, µm
τ	shear stress, MPa
τ_a	solid-to-solid shear stress, MPa
τ_l	solid-to-fluid shear stress, MPa
A	relative contact area, -
h_l	mean film thickness, µm
V_R	roll velocity, m/min
V_S	strip velocity, m/min
m^C, m^T	Coulomb limited Tresca law parameters, -
σ_x, σ_y, σ_z	stress in axis directions, MPa
F_Y	rolling force , N/mm
S_F	forward slip, -
L_e	roll-bite length, mm
R_r	roll radius, mm
σ_1, σ_2	strip entry and exit tension, MPa
$t_{s,1}$, $t_{s,2}$	strip entry and exit thickness, mm

1. Introduction

The general framework of this article is in the field of cold rolling of flat products. This paper presents a new experimental system which uses ultrasonic sensors to perform measurements at the interface between the work rolls and the strip.

Cold rolling is a mechanical process which incorporates many complex mechanisms at different scale levels. At the macroscopic scale, the interaction between plastic deformations of the strip and thermo-elastic deformations of the rolls can lead to flatness defects which are very detrimental to further metal processing such as stamping. This coupling between the strip and the roll becomes even more important as the strip gets thinner [1].

Phenomena taking place locally in the roll bite, at the microscopic level, also have an important impact on the rolling-stand behaviour. The roll gap is operating in the mixed lubrication regime where both solid-to-solid contact between the asperities of the rolls and the strip as well as solid-to-fluid contact occur. This regime allows a lower friction level than in the boundary regime and a controlled strip roughness which cannot be achieved in the hydrodynamic lubrication regime due to strip roughening [2]. In the mixed lubrication regime, interactions between the asperities of the rolls and the strip and their impact on the lubricant flow play a key role in the generation of shear stress in the roll bite. This, in turn, has an effect on the pressure profile, the rolling load and therefore the roll deformations.

If the macroscopic and microscopic phenomena mentioned above are not well mastered, they may induce strip shape defects, strip thickness inhomogeneity or a non-optimal strip roughness. To control the process, several measurements are usually carried out on industrial rolling mills. Strip thickness sensors at entry and exit of the stand are used in conjunction with hydraulic actuators to react to strip changes. Flatness measuring rolls are commonly located at the exit of the last stand to assess the quality of the strip. Also, macroscopic data accounting for the global behaviour of the roll bite such as the rolling load and the forward slip (the relative velocity between the roll and the strip

at the exit of the contact zone) are continuously recorded to estimate the friction level within the roll gap.

Nonetheless, all these measurements are made outside of the roll bite. A better control strategy could be achieved by monitoring phenomena within the contact itself with roll gap sensors. To move towards that goal, a European project RFSR-CT-2009-00008 [3], aiming at measuring friction, heat transfers and lubricant film thickness has been undertaken.

This paper presents the development of an ultrasonic sensor suitable for online measurement in a pilot cold rolling mill. The transducer is based on the reflection of an ultrasonic wave from the interface between the roll and the strip. The proportion of the reflected wave depends on how much solid contact there is and the thickness of the lubricant film.

Ultrasound has long been used as a non-destructive technique to detect defects within solid bodies [4]. More recently, it has been used in the field of tribology to investigate contact between rough surfaces [5] and measure continuous thin lubricant layers in a number of studies, such as those looking into journal bearings and mechanical seals [6,9].

This technique is now used for the first time in cold rolling where direct measurements at the roll-strip interface are very challenging. This is due to the extreme stresses involved (up to 1000 MPa), the small contact length (~5-15 mm) compared to the roll radius (50-500mm), the heat generated by the plastic deformation on the strip on such small distance, the roll speed (up to 500 m/min in the tests), the stand vibrations, etc.

Direct measurements in the roll bite have already been achieved in previous studies through direct pin friction sensors [10,12]. These were used to measure contact stresses. Even though such type of system has brought an essential insight into rolling mechanics since the 1930's, the presence of the pin marks the strip and influence contact conditions in the roll gap. This system is therefore not applicable for daily use to industrial applications.

Within the same European project, [13] have used optical fibre inserted 2 mm underneath the roll surface to measure roll strain in order to deduce roll-strip contact stresses. As in [13], the technique presented in this paper is only semi-invasive; some adaptation of the work roll is required to fit the sensors. However the rolling surface is unaltered since the sensors are not directly in contact with the strip. Using ultrasonic sensors, it is possible to measure the roll-bite length, the strip thickness variation as well as the roll deflection and stresses. Moreover, lubricant film thickness, which plays a key role in the process efficiency, is also measured. The present paper focuses on roll-bite length and strip thickness measurements. The other type of results is discussed in subsequent publications.

The first section of this paper gives the theoretical background and presents the ultrasonic measurements achieved during the testing of the sensor on a pilot rolling mill operated by ArcelorMittal. Experimental data is then compared to numerical results obtained with MetaLub, a slab-method software able to account for mixed contact conditions in cold rolling. The main features of this simulation tool are described in section 4, and the comparison with experimental measurements is presented in section 5.

2. Background

The nature of ultrasound is such that when it reaches an interface between two different media, a proportion of the wave is reflected and some is transmitted (see Figure 1 – a). The amplitude of the reflected signal compared to the initial wave, known as the reflection coefficient *R*, depends on the acoustic dissimilarity of the interface materials. Reflection coefficient can be quantified by the well-known equation [4]

$$R = \frac{z_2 - z_1}{z_1 + z_2} \tag{1}$$

where z_1 and z_2 are the acoustic impedance (given by the product of the density – ρ – and the speed of sound – c) of the media on either side of the interface.

By using this principle, flaws within materials can be detected through their ultrasonic reflection (see Figure 1 – b). Moreover, their position is obtained from the speed of sound within the media and the time difference between the emitted signal and its reflection Δt. This distance measurement, known as the time-of-flight (ToF), has been used by engineers for a long time and is well understood.

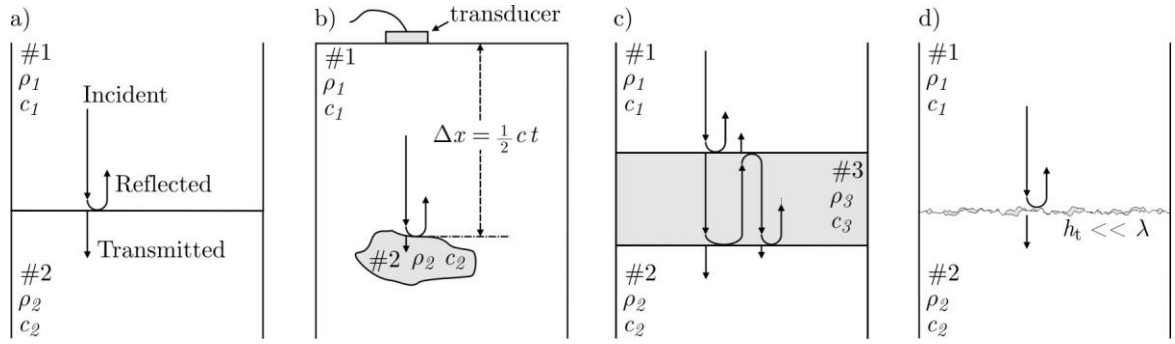

Figure 1. a) Schematic view of an ultrasonic beam reaching the interface between two different media. A part of the incident wave is transmitted while the rest is reflected. b) Working principle of the ToF method used to detect flaws within material. c) Consecutive ultrasonic reflections for a three-layered medium. d) Behaviour of a three-layered interface when the mean thickness – h_t – of the intermediate media is much lower than the wavelength – λ – of the ultrasonic pulse: a unique reflection occurs.

When ultrasound is sent through a multi-layered system, a reflection occurs at each interface while the remaining part of the signal crosses the interface (see Figure 1 – c). Very thick layers (of the order of mm) can be measured with the ToF technique. Smaller thickness measurements are unfeasible with ToF since reflected pulses from either side of the layer overlap in the time domain.

If the wavelength of the ultrasonic pulse is large in comparison to the thickness of the layer, then the layer acts as a unique reflector (see Figure 1 – d). The system can be treated quasi-statically and a spring-model approach is used. The properties of this interface depend on the properties of the embedded layer as well as the material on either side. Then, the equation (1) becomes [14]

$$R = \frac{z_1 - z_2 + i\omega\left(z_1 z_2 / K\right)}{z_1 + z_2 + i\omega\left(z_1 z_2 / K\right)} \tag{2}$$

where ω is the angular frequency of the wave and K the embedded layer stiffness.

Real and imaginary parts are obtained from equation (2). Equation (3) gives the reflection coefficient vector when identical materials are used on either side of the interface

$$|R| = \frac{1}{\sqrt{1 + \left(2K / \omega z\right)^2}} \tag{3}$$

In the following sections, it is shown how the ToF method and the reflection coefficient are used to infer roll-bite length and strip thickness variation along the contact zone.

3. Experimental setup

Experiments were carried out on a pilot rolling mill based at ArcelorMittal's research campus in Maizières-lès-Metz (France). The ultrasonic measurement instrumentation consisted of two piezoelectric transducers, an ultrasonic pulser/receiver (UPR) and a data acquisition system (DAQ). These different components are described in the following paragraphs. A general sketch for the data acquisition system is shown in Figure 2.

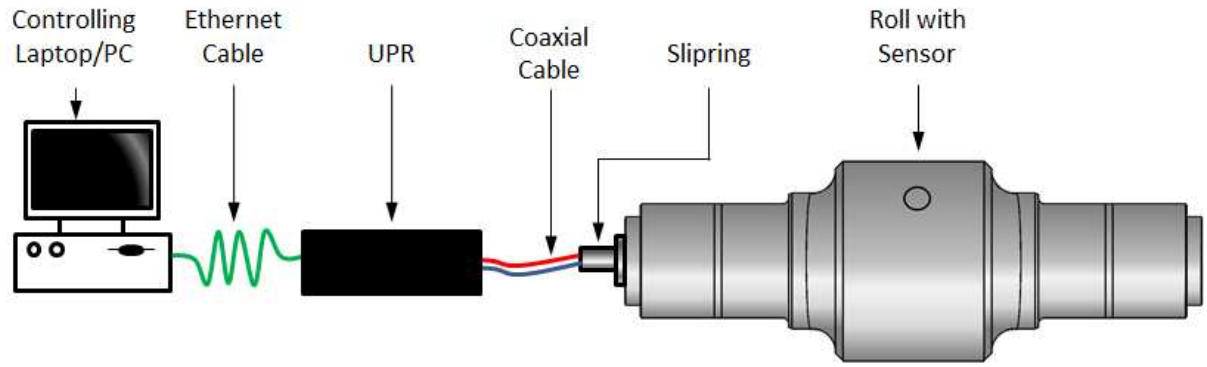

Figure 2. Ultrasonic data acquisition system overview. An ultrasonic pulser/receiver controlled by a computer is used to send and receive signals from ultrasonic sensors through coaxial cables connected to an instrumented plug in a roll.

3.1. Ultrasonic sensors

Separate shear and longitudinal piezo transducers are used. The transducers are simple bond-on piezo elements with 10 MHz centre frequency as they provide good penetration into steel and a clear distinct signal.

Original elements, initially disc shaped with a diameter of 7 mm, are modified to form narrow strips (see Figure 3 – a). They are bonded to the transmission material using an adhesive that also acts as a couplant (see Figure 3 – b). Piezoelectric elements are then protected with a layer of epoxy (see Figure 3 – c) that also damps the sensor suppressing sensor ringing. The sensing area of the resulting system is approximately the same size as the sensor.

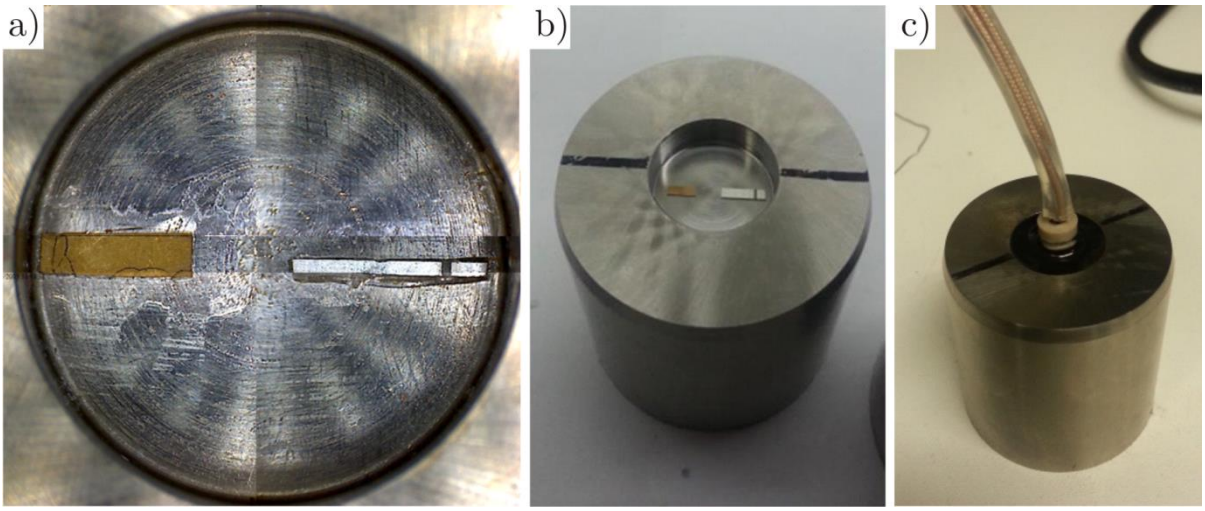

Figure 3. Metal plug, used in cold rolling testing, at various stages of instrumentation. a) Shear (left) and Longitudinal (right) sensors bonded to the top of the metallic part. b) Global view before sensor connection to the wires and epoxy covering. c) State of the plug before roll fitting.

The transducers are mounted to a metal plug which is then pressed into a hole drilled within the work roll, such that the generated ultrasonic pulse is reflected from the external surface of the roll. The plug and roll surface are then ground in a single operation. Wires to the transducers are extracted through access holes drilled radially and along the axis of the roll, and connected via a slip-ring mounted directly to the end of the work roll, as shown in Figure 4.

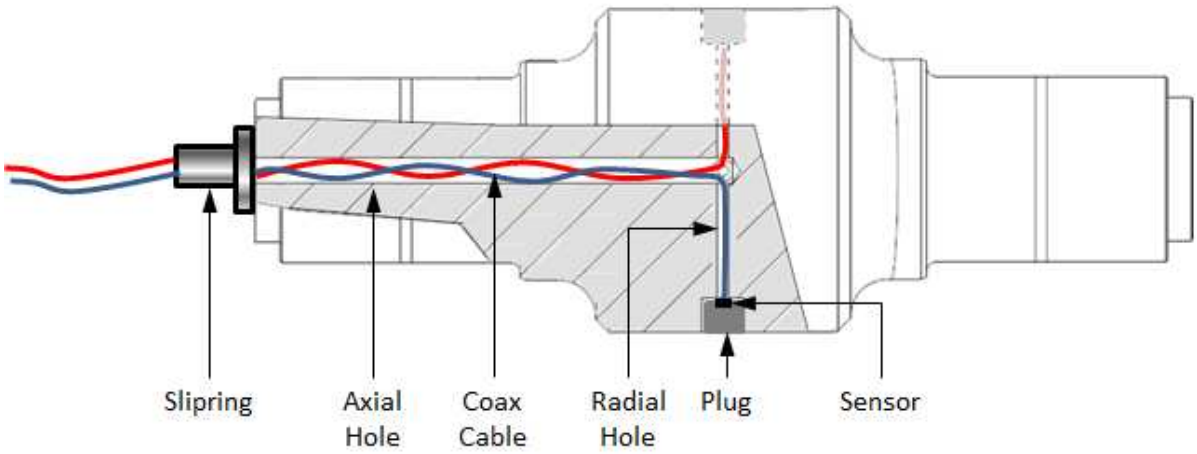

Figure 4. Section view of roll showing instrumented plug installation and wire routing.

3.2. Ultrasonic pulsing and receiving instrumentation

To generate an ultrasonic pulse a voltage signal is used to excite the piezoelectric transducers and thus produce an ultrasonic wave. Returned waves reflected from an interface are captured by the reverse of this process. The voltage signal used typically takes the form of an inverted top hat. Signals of magnitude ~50 V were used in the following tests. The signal width defines its frequency which in-turn influences the frequency content of the ultrasonic pulse produced. For best efficiency the pulse width (or period) should be set to half the transducer's centre frequency. This means energy is transferred to the transducer at its natural resonant frequency which can increase the signal amplitude by 12 dB or more compared to a spike pulse of the same amplitude (3).

The Pulse Repetition Frequency (PRF) is the rate at which ultrasonic pulses are sent out. The system used is capable of 100kHz global PRF which is split between the number of channels in use, so 2 channels will have a maximum PRF of 50kHz, 3 channels have a maximum of 33.3kHz and so on. The hardware switches between pulsing and receiving modes, it cannot do both simultaneously. This means that it is necessary to pulse, switch to receiving mode and wait for the response, before switching back to send another pulse. The length of the ultrasonic path and the speed of sound of the transit material define the minimum length of this wait. The maximum achievable PRF is therefore a function of the hardware capability, number of sensors and ultrasonic transit time. The PRF used was 7.5 kHz per channel, a limitation resulting from the plug length.

In order to match the returned signal amplitude to the digitiser range the incoming signal is amplified prior to digitisation. This is done in two stages, firstly the signal passes through a fixed preamplifier, then a variable *Gain* amplifier. Amplification only ensures the best use of the digitiser resolution, reducing quantization error. As it also amplifies any noise, there is no gain in the signal to noise ratio (SNR). Improved signal to noise ratio is achieved by increasing the incident wave amplitude, and by removing sources of electromagnetic interference (EMI) through adequate screening of the electronics and cabling. The amplification used varied between tests and sensors.

After amplification the returned signal was then digitised with a 12-bit 100 MHz digitiser. The Nyquist rate (Chen, 2001) defines a lower boundary of the sampling rate required for alias-free signal digitising. This stipulates a sampling rate of greater than twice the highest frequency component of the waveform. This represents a theoretical ideal for continuous signals, a more commonly used rule of thumb when dealing with pulse based ultrasonic signals is to use a digitising rate at least a factor of ten greater than the wave centre frequency. For example, the 100MHz digitiser used is sufficient to accurately reconstruct a 10MHz pulse.

The digitised signal was passed to a PC for processing. The signal was processed in real-time using bespoke software custom written in National Instruments LabVIEW. The completed software was capable of saving the raw data to disk while also processing the data in real-time, including the calculation of the signal Fast Fourier Transform (FFT), reflection coefficient and interface stiffness.

The combination of high-pulsing voltage, short rise and fall times, high pulse repetition rate, low response voltage and the high rate of digitisation required made typical data acquisition equipment unsuitable. Instead an FMS100 produced by Tribosonics Ltd was used. This is a specialised ultrasonic pulse generation and digitisation piece of equipment which takes the form of a set of PCI cards mounted within an industrial PC chassis. The hardware is also controlled with custom software written in NI LabVIEW.

3.3. Rolling mill

Ultrasonic measurements are made during rolling experiments carried out on a pilot mill. This mill (see Figure 5 – a) is a 2-high-stand configuration where tensions, rolling speeds, forces and lubrication conditions representative of industrial applications are achievable.

Once the metal plug is pressed into the roll, the roll surface is grinded to avoid any geometrical discontinuity between the roll and the plug. The roll surface around the plug position after grinding is shown in Figure 5 – b and the plug position is barely visible.

During the tests, very slight marks were left by the plug on the strip. They are due to the large contact pressure involved in these tests (the numerical model predicted maximal pressure values between 450 and 800 MPa for the different tests presented in this paper).These small marks are acceptable for the testing conducted on the pilot mill but they prevent the present system to be used on an industrial mill on a daily basis since they would be detrimental to further metal processing such as stamping. However, perturbations due to the presence of the plug on the rolling condition are expected to be small. Indeed, the sensing area is small (<5mm diameter) in comparison to the plug diameter (40mm) and located in the centre of the plug away from the edges. It is therefore expected that while the edges of the plug may have resulted in some strip marking at higher pressures, that the centre of the plug and therefore ultrasonic readings are unaffected.

Figure 5. a) ArcelorMittal pilot mill where ultrasonic sensors were tested. b) Roll surface, around the plug containing the ultrasonic sensors, after grinding. The geometrical discontinuity is reduced and the plug position is barely visible.

4. Ultrasonic measurements

Sensors fitted in the work roll emit signals towards the outer surface of the roll. When the wave strikes a part of the roll surface out of the roll bite, almost all of the wave is reflected back (see Figure 6). This is because the acoustic impedance of air or oil is much lower than the one of the solid material. For instance, at a steel-air interface the amplitude of the reflected wave is 99.98% of the incident wave [15].

Once the ultrasonic wave reaches the roll bite, a part of the signal is transmitted through the interface while the remaining part is reflected back to the transducer (see Figure 6). Since the lubricant film thickness on either side of the strip is small (in the order of μm) compared to the ultrasonic wavelength (0.58mm in steel at 10MHz), a single reflection occurs at each roll-strip interface. The wave transmitted into the strip is then partially reflected back at the interface with the bottom roll. Finally, a part of this pulse crosses the upper roll surface to reach the piezo-element.

Strip thickness and reflection coefficient are obtained from these different signals as explained in the following paragraphs.

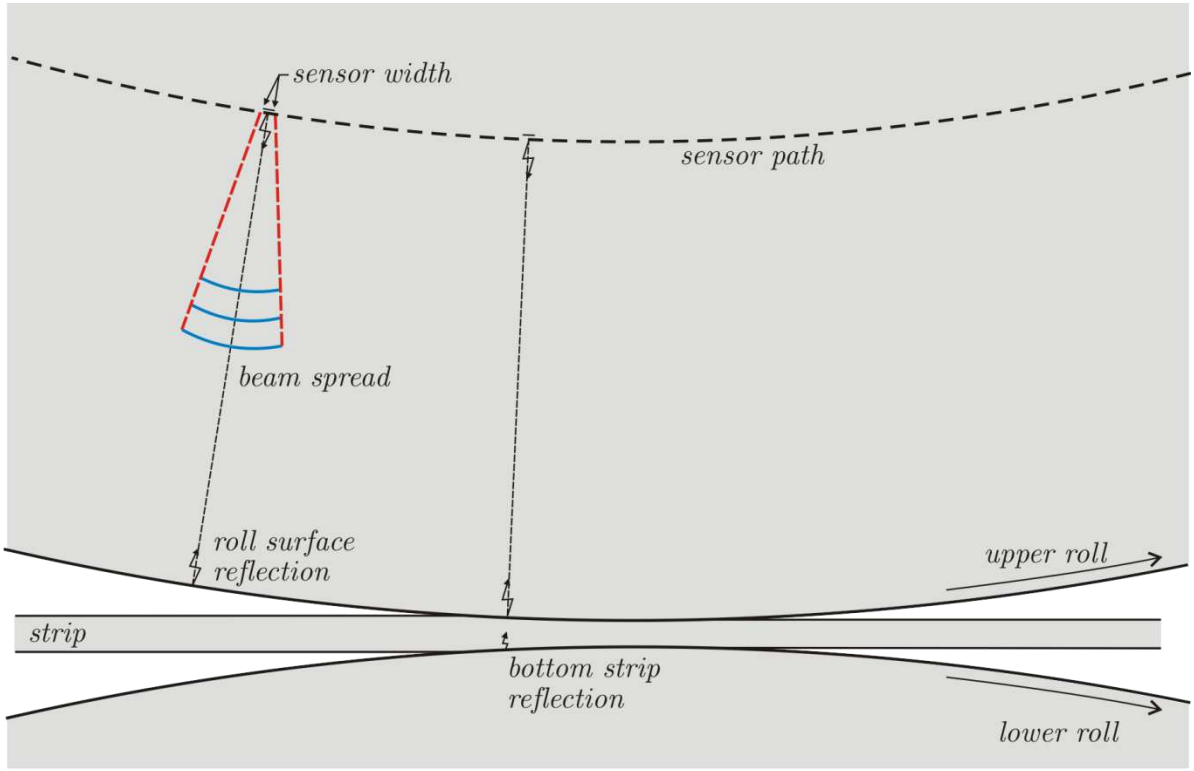

Figure 6. Ultrasonic reflections in cold rolling depending on the sensor position along its path. The initial distance d_0 (unloaded case) between the sensor and the roll surface is 35 mm. Except for the beam spread, the proportions are accurate for a 2.8 mm strip thickness undergoing a reduction of 40%.

4.1. Strip thickness

The signals reflected back to the sensors as a function of time (A-Scan) are shown in Figure 7 for two sensor positions: outside and inside the roll bite. These graphs represent reflections from different interfaces, with the time difference between the pulses being the result of the respective differences in wave path length. When the sensors are outside the roll bite, a single reflection coming from the roll surface (steel-oil or steel-air interface) is observed (see Figure 7 – a). Once the sensors are in the roll bite, the signal amplitude of the first roll reflection decreases, since a part of the pulse is transmitted through the strip, and a reflection from the lower face of the strip being rolled was observed (see Figure 7 – b).

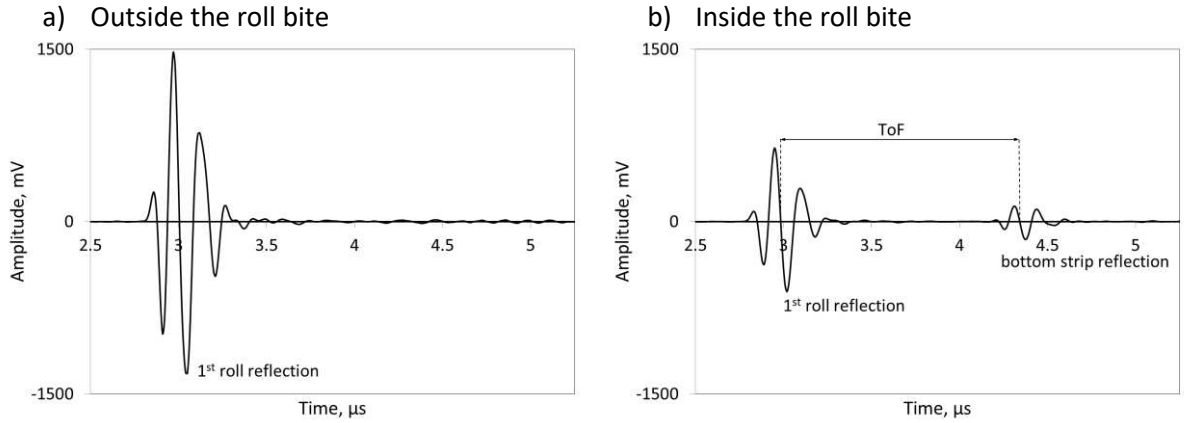

Figure 7. Ultrasonic responses measured, outside (a) and inside (b) the roll bite, with the shear sensor.

As clear reflections from both top and bottom surfaces of the strip are captured during rolling, the strip thickness could be measured using the time-of-flight technique. The ToF was determined with a zero-crossing method. This consisted of measuring the time between two similar points on successive reflections. These points are taken as the intersection of the curve located between the maximum peak and the following minima with the horizontal axis (see Figure 7 – b).

The time difference obtained with zero-crossing is not only due to the distance between the top and bottom part of the strip (thickness), it is also affected by phase shift and the acoustoelastic effect. Indeed, when a reflection occurs at a contact between two components both the amplitude and the phase are affected by contact conditions [16]. Therefore phase shift induces a variation of

the signal shape which may give inaccurate measurements with ToF. However, phase variations observed in experimental measurements are small and therefore neglected for this study.

Acoustoelasticity is the stress dependence of acoustic wave velocity in an elastic media: the speed of ultrasound increases when stress in the material increases [17, 18]. This change in the speed of sound results in a different ToF possibly resulting in an error in the thickness calculation. However, in the present case, the effect is only slight and the error it will induce is likely to be very small (<1%) and so it has been disregarded.

Strip thickness is computed upon signals measured with shear sensors. Indeed, as shear waves travel at approximately half of the speed of longitudinal waves, it is possible to gain almost twice the resolution in strip thickness using the same digitising rate. Moreover, shear waves are less sensitive to acoustoelastic effect. The speed of sound for bulk shear waves in the plug when the material is unloaded is c = 3252.68x10^3 mm/s.

4.2. Roll bite length

For a given position of the sensor, the reflection coefficient is computed from the Fast Fourier Transform for the first reflected pulse $A_{meas}(t)$ and a reference signal $A_{ref}(t)$. The reference is taken as a reflected signal measured outside the roll bite with an air interface. After the conversion of $A_{ref}(t)$ and $A_{meas}(t)$ in the frequency domain, the amplitude of the reflection coefficient $|R|$ is obtained as the ratio between these two signals at the frequency f_{max} where $A_{ref}(f)$ is maximum.

$$|R| = \left| \frac{A_{meas}(f)}{A_{ref}(f)} \right|_{f = f\,\max,\, ref} \tag{4}$$

As the roll rotates and the ultrasonic sensor passes across the rolling interface, a profile of the reflected pulse amplitude can be built up (see Figure 8). A pulse amplitude drop is observed, as expected. This is due to the ultrasonic wave being transmitted through the rolling interface, and therefore a smaller part of the wave being reflected.

On the left part of the curve reflection coefficient values are close to 1. It means that most of the incident signal is reflected back to the transducer. Then, the response drops with a linear gradient to reach a value close to 0.1-0.2. At this stage, the sensor beam is facing the roll bite and reflection to the sensor is low. Finally, the reflection coefficient increases linearly to reach initial values close to 1 and the sensor is out of the roll bite. The actual location of the entry and exit of this roll bite occurs at some point along these two slopes, likely to be the mid-point (i.e. |R| = 0.5).

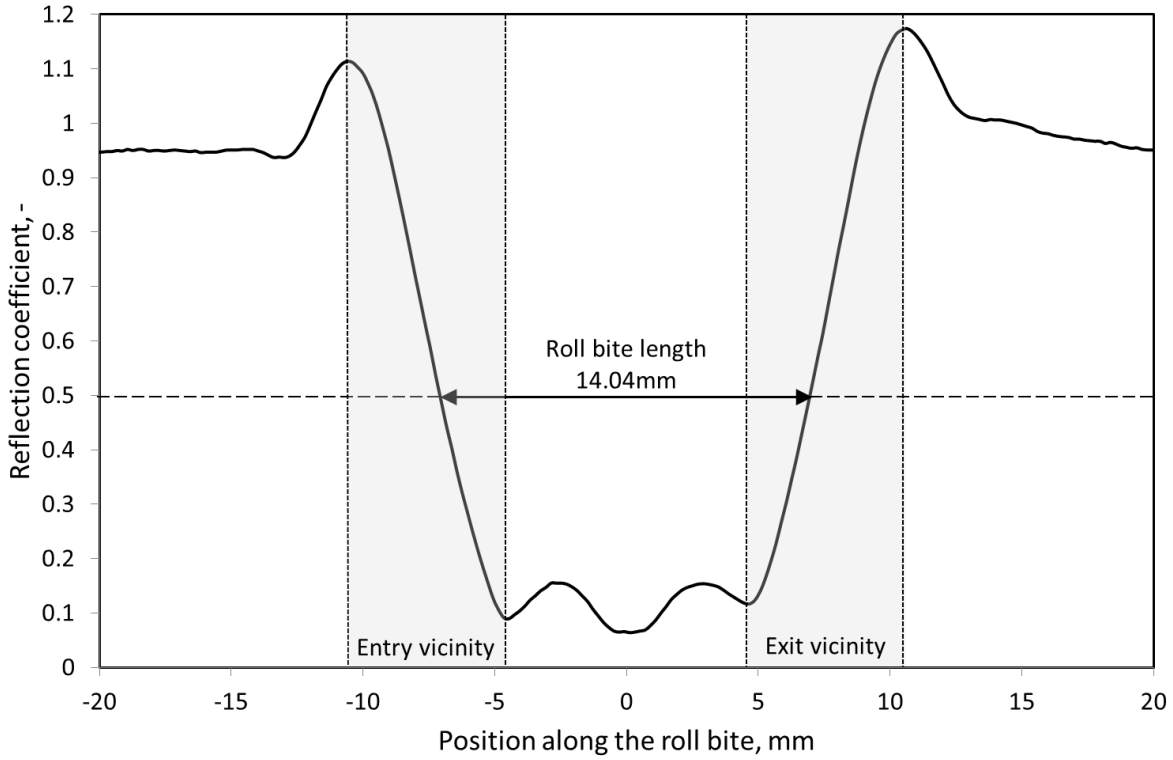

Figure 8. Example of some reflection coefficient measurements across the roll bite with longitudinal sensor. The amount of reflected wave drops as the sensor beam reaches the contact zone between the roll and the strip.

Although they have no effect on the measurement being taken, it is interesting to note that peaks with a reflection coefficient of >1 can be observed near to the entry and exit of the roll bite, as shown in Figure 8. These peaks occur in these positions regardless of roll bite length or rolling conditions. It is suspected that they result from an interference effect.

Reflection coefficient profiles corresponding to 4 strip elongation values are plotted in Figure 9. During the experiments the strip elongation has been increased stepwise, from 10% to 40%, while rolling one coil, the other rolling parameters being kept constant. The time span of all these steps is approximately 40 seconds which is enough to achieve steady state conditions. Steady state is reached once macroscopic parameters such as the rolling load and the forward slip have attained stable values. The obtained reflection coefficient profiles become wider as strip elongation increases. A larger strip elongation induces a larger roll-bite length for two reasons. The first reason is geometrical: the arc of the roll intercepted by the strip becomes larger as the strip elongations increases. The second one is due to the larger rolling load inducing roll deformations leading to a larger contact length. As in previous section, the roll-bite length is estimated by measuring the distance between two consecutive points on the reflection coefficient profile, at a threshold value of 0.5.

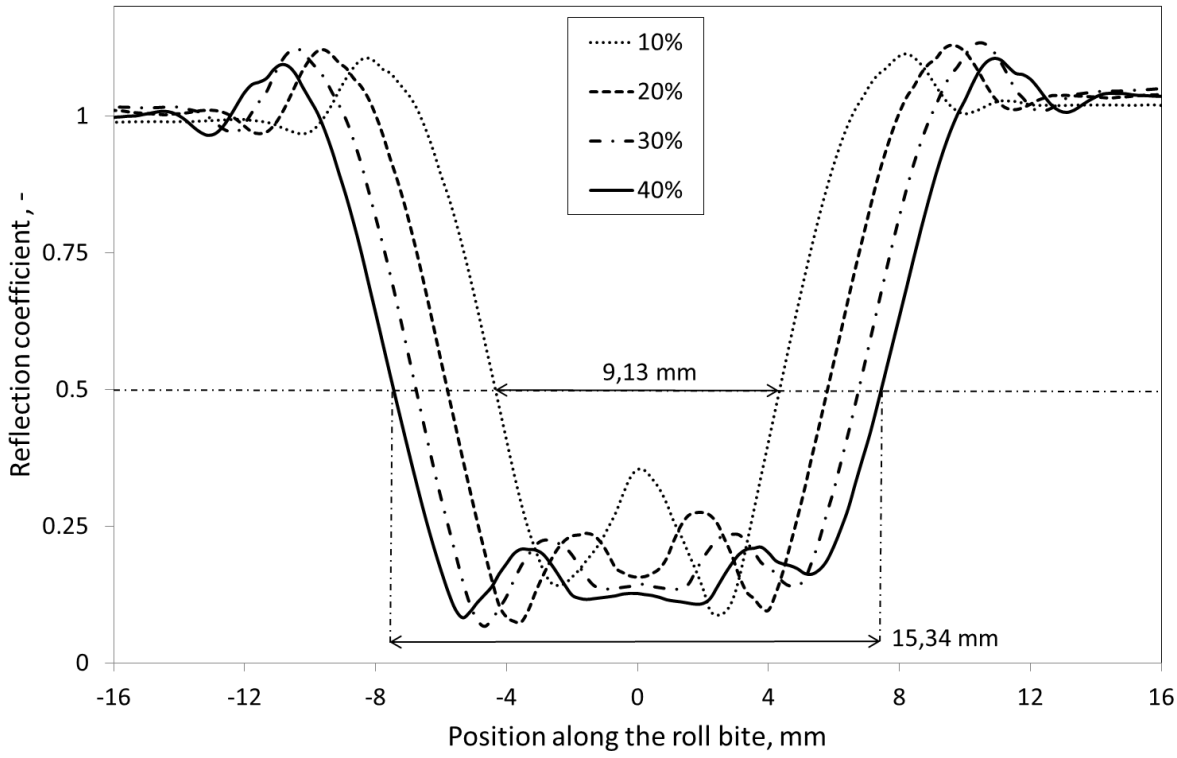

Figure 9. Reflection coefficient computed upon ultrasonic measurements made with longitudinal sensor for various strip elongations.

Contact length is also determined continuously while strip elongation is increased during rolling. The variation observed in the transient regime is plotted in Figure 10 along with strip elongation. These two curves clearly exhibit the same pattern. While strip elongation increases from 5% to 40%, contact length varies from 6.7mm to 15.1mm.

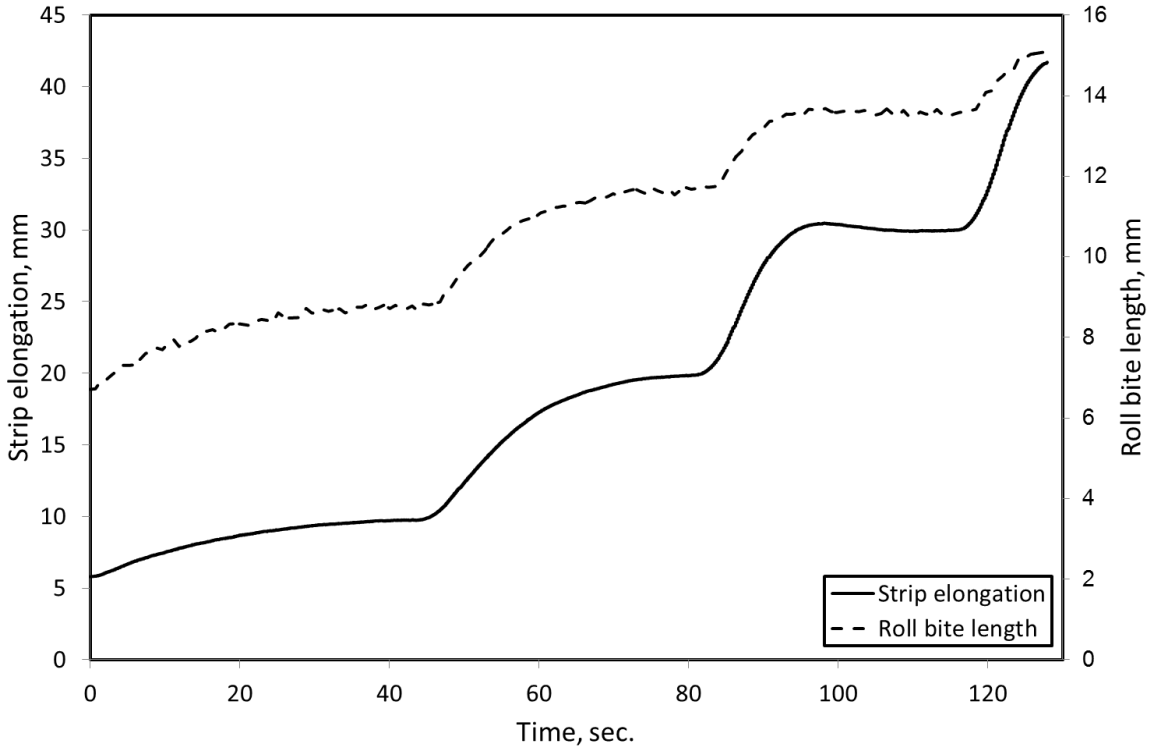

Figure 10. Contact length measured ultrasonically in the transient regime, and elongation measured by the mill coiling system (pulse generators measuring the velocity of the strip at the entry and the exit of the roll bite allowing to determine the strip elongation).

No independent measurement of the roll bite length exists to validate the ultrasonic results against Numerical modelling are then completed to validate the ultrasonic results. The numerical model used in this study is presented in the next section.

5. Numerical modelling of cold rolling conditions measured during ultrasonic testing

As mentioned in the introduction, a cold rolling stand is a highly non-linear system which incorporates many complex mechanisms at different scale levels such as the stand elastic deformations, roll-flattening, elastoplastic deformations of the strip, interactions between the asperities of the rolls and the strip, lubricant flow in the roll bite, etc.

Over the years, many numerical techniques have been developed to get a better understanding of the phenomena involved in the process. The use of these simulation tools help process engineers to tackle issues such as roll deformations and strip shape defects, lubrication optimisation, etc.

Montmitonnet [1] gives a review of rolling numerical models. Different numerical approaches, either 1, 2 or 3D have been used to model cold rolling, depending on the required precision and relevant input parameters. 3D models are usually used to study flatness defects. When flatness defects can be neglected, simpler 2D models can be used, especially when thickness reductions are small. 1D models are sometimes sufficient and cheaper in terms of computational time; in the case of flat products, ”a 1D model is perfect for a ratio between the length of the roll bite and the strip thickness higher than 3” [1].

To validate the experimental measurements, numerical simulations are conducted with MetaLub [24 - 25], a 1D simulation code designed to model mixed lubrication conditions occurring in cold rolling. The main features of this numerical tool used in this study are described in the paragraphs below. The results are then compared to experimental data in the next section.

5.1. Strip model

Like most cold rolling simulation codes dealing with mixed lubrication conditions, MetaLub is based on the slab method [19- 21]. This methodology only accounts for principal stresses in the strip, neglecting shear. For each computed result (stresses, plastic strain, velocity, etc.) only one single value is associated with each position along the roll bite.

The hardening law of the material rolled during the testing corresponds to equation (5). Numerical parameters are obtained by fitting plane strain compression test measurements.

$$\sigma_y\left(\bar{\varepsilon}^p\right)=\left(451+152\ \bar{\varepsilon}^p\right)\left(1-0.3\exp\left(-9.13\bar{\varepsilon}^p\right)\right) \qquad [\mathrm{MPa}] \tag{5}$$

5.2. Lubricant flow computation

Lubricant pressure is computed with an average Reynolds equations developed by Wilson and Marsault [22-23]. This equation includes two flow factors to deal with the asperity presence on the fluid flow when large values of relative contact area occur between asperities of the strip and the rolls.

Lubricant piezo-viscosity dependence can be accounted for with several laws. For the simulations conducted in this study, an improved version [29] of a modified WLF equation [30] is used:

$$\log\left(\frac{\eta}{\eta_g}\right)=\frac{-C_1\left(T-T_g(p_l)\right)F(p_l)}{C_2+\left(T-T_g(p_l)\right)F(p_l)} \tag{6a}$$

$$T_g(p_l)=T_g(0)+A_1\ln(1+A_2p_l) \tag{6b}$$

$$F(p_l)=(1+B_1p_l)^{B_2} \tag{6c}$$

This equation gives the evolution of the lubricant viscosity η as a function of the lubricant pressure p_b, the temperature T and the glass transition temperature T_g where A_1, A_2, B_1, B_2, C_1 and C_2 are parameters having to be identified experimentally.

Rolling cases discussed in the present paper are lubricated with pure oil. Numerical parameters corresponding to this oil are listed in Table 1.

A_1 [°C]	A_2 [MPa^{-1}]	B_1 [MPa^{-1}]	B_2 [-]	C_1 [-]	C_2 [°C]	η_g [MPa.s]	$T_g(0)$ [°C]
49.64	0.000365	0.00578	-0.565	16.11	26	1 000 000	-85.96

Table 1. Numerical parameters obtained by fitting experimental measurements carried out on the pure oil used during rolling trials.

Asperity crushing is a critical phenomenon in the mixed lubrication regime since it determines the amount of solid-to-solid contact between the strip and the work-rolls. In the simulations, that aspect is traduced by the relative contact area *A* and computed thanks to semi-empirical laws developed by Wilson and Sheu [26] or Sutcliffe [27]. These analytical crushing laws connect the relative area of contact *A* to the non-dimensional effective hardness (*H*) and the non-dimensional bulk strain rate (*E*).

In the case of strip rolling, Marsault [22] defined a law which links the evolution of the three previous variables (*A*, *E* and *H*) inside the roll bite. This equation was established considering a smooth rigid tool and a rough strip surface. To overcome this issue, the composite roughness R_q is currently used when needed.

$$R_q = \sqrt{R_{q,strip}^2 + R_{q,roll}^2} \tag{7}$$

where $R_{q,strip}$ and $R_{q,roll}$ are the quadratic roughness of the strip and the rolls.

In the simulations, Wilson and Sheu's asperity crushing law is used and asperity shape is assumed to be triangular. Arithmetic roughness was measured on the upper roll and on the strip before rolling. Measurements are very similar for the two test conditions discussed here. For triangular asperities, quadratic roughness is inferred from arithmetic roughness using the following equation

$$R_{q,strip} = \frac{2}{\sqrt{3}} R_{a,strip} \tag{8}$$

Composite roughness R_q is then determined. Finally, the half distance between asperities (*ll*) is computed assuming an asperity slope of 7° which is realistic for this type of surface.

$R_{a,roll}$ [µm] (measured)	$R_{q,roll}$ [µm]	$R_{a,strip}$ [µm] (measured)	$R_{q,strip}$ [µm]	R_q [µm]	asp. slope [°] (assumption)	*ll* [µm]
0.616	0.77204	1.505	1.8862	2.0381	7	24.553

Table 2. Arithmetic roughness - R_a - measured on the upper roll and on the strip before rolling. Quadratic roughness R_q is inferred from these measurements assuming triangular asperity shape. The assumed slope of 7° gives a half distance between asperities *ll* = 24.553 [µm].

5.3. Deformable work-roll

In the simulations conducted in this study, deformations of the roll are computed with Jortner's formulation [28]. In that case, the deformed shape is the linear superposition of several loading cases caused by diametrically opposite normal forces. These normal forces are the integration of the interface pressure profile projection on the roll-mesh. This method is able to represent large flat zones encountered in heavily loaded configurations. For rolls made of steel, usual Young's modulus and Poisson's ratio values of 210 000 MPa and 0.3 are used. Roll diameters in the trials were 391 mm.

5.4. Roll/strip interface: friction model

The interface shear stress τ, defined at each point of the roll bite, is computed by the classical sharing law which determines upon the solid-to-solid (τ_a), the solid-to-fluid shear stresses (τ_l) and the relative contact area A.

$$\tau = A\,\tau_a + (1 - A)\tau_l \tag{9}$$

The solid-to-solid friction stress is given by the following relation

$$\tau_a = \min(m^C|\sigma_n|, m^T k) \tag{10}$$

Where σ_n and *k* are the normal stress and the yield shear stress respectively. This law requires the definition of two new parameters m^C and m^T. They rely on the strip rolling conditions and have to be adjusted by comparing numerical results to experimental data. Since these parameters account for many complex mechanisms, they cannot be determined beforehand.

In this study, Coulomb's coefficient is adjusted to match rolling load and forward slip (defined as the relative difference between work roll and outlet strip velocities). A constant ratio between m^T and m^C of 2.6 is chosen ($m^T = 2.6\, m^C$) [24].

The solid-to-fluid shear stress (τ_l) is a function of the lubricant viscosity (η) and pressure (p_l), the relative contact area (A), the mean film thickness (h_l) and the sliding velocity between the rolls and the strip ($V_R - V_S$).

$$\tau_l = \eta \frac{(1-A)(V_R - V_S)}{h_l} \tag{11}$$

5.5. Thermal effect

The software has an option for a simplified temperature prediction neglecting conduction and heat transfer (i.e. adiabatic) see [24]). Nevertheless, thermal effects are neglected in this study because the investigation does not require it. Therefore, the temperature is assumed to be constant throughout the roll bite. Lubricant temperature is set to 60°C matching the lubricant temperature sprayed on the rolls and strip.

5.6. Resolution method

The resolution method is based on two imbricated shooting loops [22]. The inner one acts on the lubricant flow to get a null fluid pressure at the roll bite exit whereas the outer one acts on the inlet strip speed to match a given strip exit tension. These imbricated shooting loops are embedded inside an iterative method, which determines the deformation and the vertical position of the rolls. Stephany [24] gives a detailed presentation of the equations.

5.7. Software results

Some of the computed results can be directly compared to the measurements usually made on industrial cold strip rolling lines (e.g. rolling force and torque, and forward slip).

Moreover, MetaLub also provides a complete set of physical fields along the roll bite, such as the interface pressure, the shear stress, the strip thickness, the relative area of contact A, the stresses σ and strains ε, etc.

Since the set of ordinary differential equations are integrated using the 4th order Runge-Kutta algorithm associated with a variable time step, the roll bite entry and exit are computed accurately. MetaLub results are therefore compared to strip thickness and roll-bite length measurements in the next section.

6. Comparison between experimental and numerical results

The following section compares the results gained both empirically and numerically.

6.1. Strip thickness

Wave reflections from the top and bottom of the strip are measured for some rolling cases and the strip thickness computed with the ToF method. The strip thickness obtained from experimental measurement in rolling test A (see Table 3) is compared to numerical results in Figure 11.

	$t_{S,1}$ -mm	elong. - %	σ_1 - MPa	σ_2 - MPa	V_R – m/min	F_y - N/mm	S_F - %
Test A	2.8	29.7	44	117	22.5	6138	4.3

Table 3. Test condition encountered in test A when measuring strip thickness variation.

In the numerical results, the first contact between the roll and the strip asperities is detected in x_1 = -11.5 mm while the roll bite exit is in x_2 = 1.626 mm. Between these two points, numerical and experimental curves are very close to each other: the maximum difference is 5%.

Experimental results also appear to give a strip thickness in excess on either side of the strip thickness profile computed with MetaLub. The reason for this is that an ultrasonic beam spreads as it propagates through a material; the wave at the extremities of the beam is travelling at an angle to the primary beam direction (see Figure 6). This means that some of the signal is returning from the roll bite, even when the transducer is not directly facing the roll bite. The signal path through the strip is therefore longer than the strip thickness thereby explaining this erroneous reading.

By measuring the roll-bite length for this test condition using the reflection coefficient curve as described earlier with a threshold value of 0.5 (the mid-point between a complete transmission of the signal and the full reflection), a length of 14.04 mm is ascertained (see Figure 8). The roll-bite length computed with MetaLub for that rolling configuration is 13.24 mm. The relative difference

between the two is small: 6%. The reflection coefficient profile can therefore be used to determine the roll-bite length.

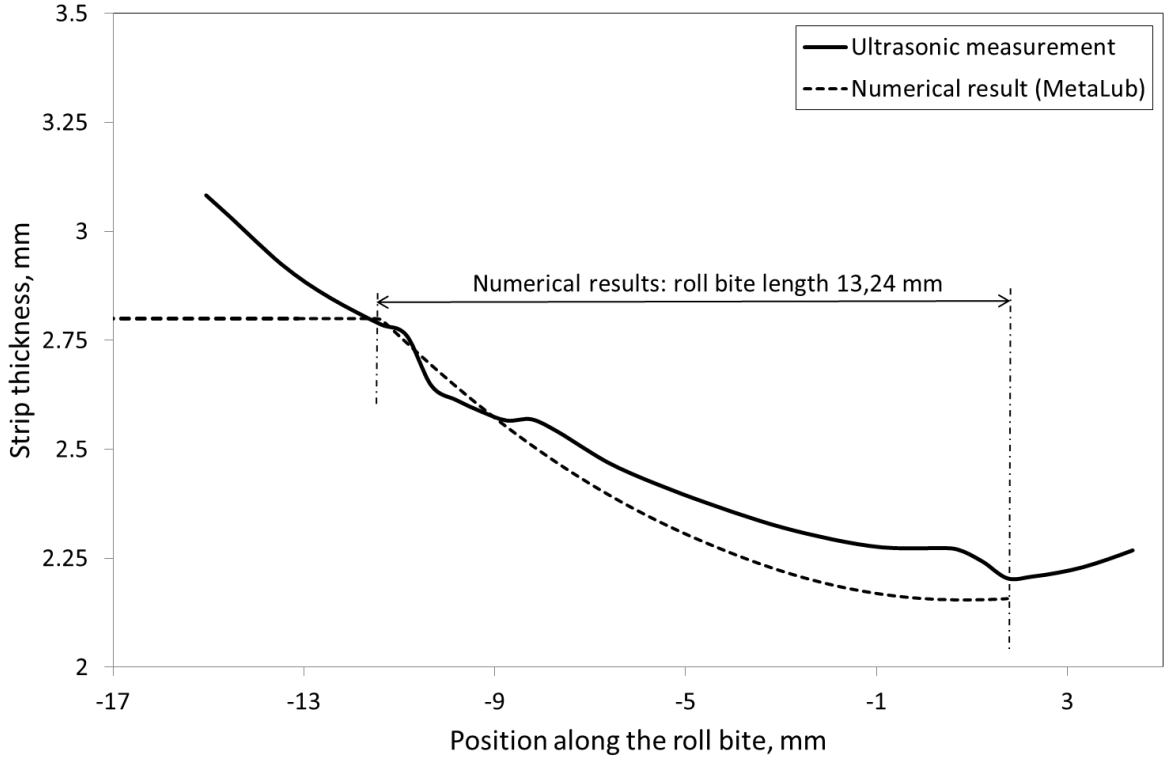

Figure 11. Strip thickness profile comparison: experimental measurements vs. numerical results. Experimental and numerical results are close to each other in terms of strip thickness variation and roll-bite length.

The next section compares the roll-bite length measured for different rolling configurations.

6.2. Roll-bite length

Measurements are made with the ultrasonic sensors for different rolling conditions where the strip elongation varied from 10 to 40%. All the other parameters are kept constant. These rolling configurations are summarised in Table 4.

	$t_{S,1}$ -mm	elong. - %	σ_1 - MPa	σ_2 - MPa	V_R – m/min	F_y - N/mm	S_F - %
Test B.1	2.8	10	38	119	97.5	3505	5.05
Test B.2	2.8	20	38	119	97.5	5300	4.65
Test B.3	2.8	30	38	119	97.5	6460	3.33
Test B.4	2.8	40	38	119	97.5	7267	2.47

Table 4. Test condition encountered in test B when measuring roll-bite length for different strip elongation.

These values correlate very well with the roll-bite length obtained with MetaLub (see Figure 12): both types of data exhibit the same trends. In all cases the model slightly over-predicts the model, with a maximum relative difference of 3% that occurs at a strip elongation of 40%. The reflection coefficient (R=0.5 as shown in Figure 8) selected as a switch to mark when the strip is in contact is somewhat arbitrary. It is clear that since there is a consistent over-estimation in the measurement that this selected value was a little too high. The relationship between the reflection coefficient and the solid-solid contact in the inlet and outlet regions is complex and depends on the nature of the partial rough surface gap, the presence of oil meniscus, and the transducer sound field. To achieve a more robust measurement would require modelling of these phenomena.

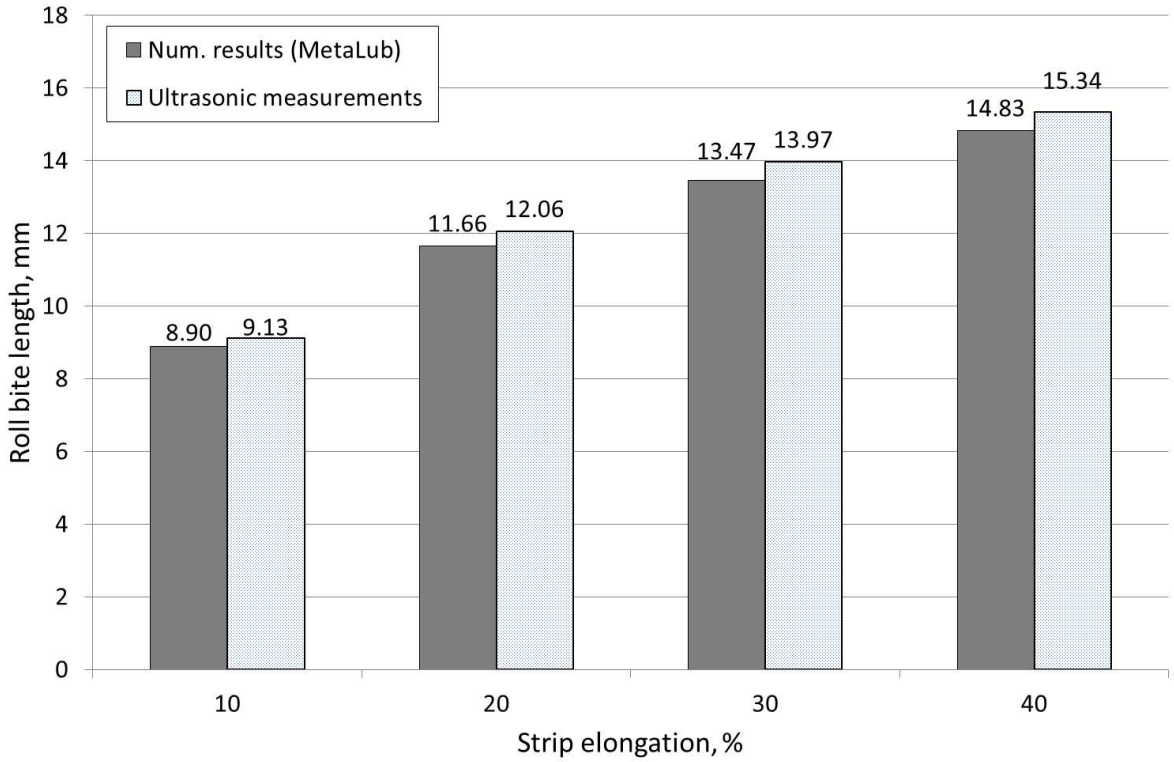

Figure 12. Roll bite length comparison: experimental measurements vs. numerical results.

7. Conclusion

Ultrasonic sensors were used on a pilot mill to carry out measurements in the contact zone between the upper roll and the strip during cold rolling of thin metal sheet. Since the lubricant layer going through the roll bite is small compared to the wavelength of the ultrasonic pulse, the roll strip interface behaves like a single reflector. The train of returned pulses obtained when the sensor was in the roll bite showed reflections from the top and bottom of the strip, the time difference between these pulses being the result of the difference in wave path length and speed of sound in the material. The strip thickness variation in the roll bite was then obtained with a simple time-of-flight technique.

As the roll rotates and the ultrasonic sensor passed across the rolling interface, a profile of the reflected pulse was built up. A pulse amplitude drop, quantified by the reflection coefficient, was observed as expected. This is due to the ultrasonic wave being partially transmitted through the rolling interface, and therefore a lower amplitude wave being reflected. This measurement enabled the entry and exit of the roll bite to be determined, and therefore contact length. This length was also measured in the transient regime when the hydraulic screw down of the mill was adjusted to change strip elongation.

Experimental measurements were compared to numerical simulations conducted independently with a cold rolling software in the mixed lubrication regime. The comparison showed that there is a good agreement between experimental and numerical results. Therefore, these two techniques validate each other and the reliability of the measurement system is proven.

The experimental methodology presented in this paper proved to be suitable for in situ and real-time measurements in the roll bite of a pilot mill. This is useful to get a better understanding of the phenomena involved in the process when conducting some testing on the pilot mill.

Currently strip thickness can be measured before the entry and after the exit of the roll bite by using X-ray systems. The approach presented here can enhance such measurements. Our system

allows us to determine the strip thickness variation within the roll bite itself in real time, which is not possible through conventional techniques. Moreover, to the best of our knowledge, there is no device capable of measuring directly the roll bite length. This shows the significance of the present approach compared to existing methods.

The weakness of the present system holds in the use of a metal plug to fit the ultrasonic sensor in the roll. Indeed, even though precautions were taken in order to reduce as much as possible the influence of the plug – such as regrinding the roll surface after pressing the plug into the roll – slight marks were observed on the strip after rolling. This is due to the large contact pressure involved in these tests (the numerical model predicted maximal pressure values between 450 and 800 MPa for the different tests presented in this paper). Therefore, the current system cannot be used as it is on an industrial rolling mill and the present work is an intermediate step proving the concept validity.

To be used on an industrial mill on a daily basis, a method that has sensors on the outside of the roll has to be developed. Once such system is available, several measurements conducted at the same time along the roll axis with different sensors would give pieces of information such as roll flattening and differential strip elongation. Therefore thickness homogeneity and differential elongation along strip width could be evaluated in real time allowing mill operators to react efficiently by changing the cooling configuration of the roll, lubricant conditions, etc.

8. Acknowledgements

Yves Carretta gratefully thanks ArcelorMittal, FRIA (Fonds pour la formation à la Recherche dans l'Industrie et dans l'Agriculture), the Walloon Region and the European Social Fund for financial support through grant First-International: convention n°1217863.

This experimental work in this paper has been performed within the framework of the European project RFSR-CT-2009-00008, which is here gratefully acknowledged for financial support.

9. References

[1] Montmitonnet P. Hot and cold strip rolling processes. *Computer Methods in Applied Mechanics and Engineering* 2006; 195: 6604–6625.

[2] Montmitonnet P. Tribologie du laminage à froid de tôles. *Revue de Métallurgie* 2001; 125–130.

[3] Legrand N, Patrault D, Labbe N, Gade D, Piesak D, Jonsson NG, Nilsson A, Horsky J, Luks T, Montmitonnet P, Canivenc R, Dwyer Joyce R, Hunter A and Maurin L. Advanced RollGap Sensors for enhanced hot and cold rolling processes. European RFCS project RFS-CT-2009-00008.

[4] Kräutkramer J and Kräutkramer H. Ultrasonic testing of material. *Springer-Verlag*, New York, 1975.

[5] Dwyer-Joyce R, Drinkwater B and Quinn A. The Use of Ultrasound in the Investigation of Rough Surface Interfaces. *ASME Journal of Tribology* 2000; 123(1): 8–16.

[6] Dwyer-Joyce R, Drinkwater B and Donohoe C. The measurement of lubricant–film thickness using ultrasound. *Proceedings of the Royal Society A* 2003; 459: 957–976.

[7] Dwyer-Joyce R, Harper P and Drinkwater B. A Method for the Measurement of Hydrodynamic Oil Films Using Ultrasonic Reflection. *Tribology Letters* August 2004; 17: 337–348.

[8] Reddyhoff T, Dwyer-Joyce R and Harper P. A new approach for the measurement of film thickness in liquid face seals. *Tribology Transactions* 2008; 51(2): 140–149.

[9] Hunter A, Dwyer-Joyce R and Harper P. Calibration and validation of ultrasonic reflection methods for thin-film measurement in tribology. *Measurement Science and Technology* 2012; 23(10): 1–15.

[10] Van Rooyen C and Backofen W. Friction in cold rolling. *Iron and Steel Institute Journal* 1957; 186: 235–244.

[11] Tieu A, Li E and Liu Y. An experimental determination of friction in cold rolling. *Tribology Series*, 2000; 38: 467–472.

[12] Lenard J. Measurements of friction in cold flat rolling. *Journal of Materials Shaping Technology*, 1991; 9 (3): 171–180.

[13] Weisz-Patrault D, Maurin L, Legrand N, Ben Salem A and Ait Bengrir A. Experimental evaluation of contact stress during cold rolling process with optical fiber Bragg gratings sensors measurements and fast inverse method. *Journal of Materials Processing Technology*, 2015; 223: 105–123.

[14] Schoenberg M. Elastic wave behaviour across linear slip interfaces. *The Journal of the Acoustical Society of America*, 1980; 68(5): 1516–1521.

[15] Drinkwater B, Dwyer-Joyce R and Cawley P. A Study of the Interaction between Ultrasound and a Partially Contacting Solid-Solid Interface. *Proceedings of the Royal Society of London A: Mathematical, Physical and Engineering Sciences* 1996; 452: 2613–2628.

[16] Reddyhoff T, Kasolang S, Dwyer-Joyce R and Drinkwater B. The phase shift of an ultrasonic pulse at an oil layer and determination of film thickness. *Proceedings of the Institution of Mechanical Engineers, Part J: Journal of Engineering Tribology* 2005; 219(6): 387–400.

[17] Egle D and Bray D. Measurement of acoustoelastic and third-order elastic constants for rail steel. *The Journal of the Acoustical Society of America* 1976; 60(3): 741–744.

[18] Chen W, Mills R and Dwyer-Joyce R. Direct load monitoring of rolling bearing contacts using ultrasonic time of flight. *Proceedings of the Royal Society of London A: Mathematical, Physical and Engineering Sciences (The Royal Society)* 2015; 471: 2180.

[19] Bland D and Ford H. An approximate treatment of the elastic compression of the strip in cold rolling. *Journal of the Iron and Steel Institute* 1952; 171: 245–249.

[20] Alexander J. On the theory of rolling. *Proceedings of the Royal Society A* 1972; 326: 535–563.

[21] Cosse P and Economopoulos M. Mathematical study of cold rolling, *C.N.R.M.*, 1968; 17: 15–32.

[22] N. Marsault, Modélisation du Régime de Lubrification Mixte en Laminage à Froid. PhD dissertation (in French), École Nationale Supérieure des Mines de Paris,1998.

[23] W. Wilson and N. Marsault, Partial hydrodynamic lubrication with large fractional contact areas. ASME - Journal of Tribology, 1998; 120: 16–20.

[24] Stephany A. Contribution à l'étude numérique de la lubrification en régime mixte en laminage à froid, PhD dissertation (in French), Université de Liège, 2008.

[25] Carretta Y, Boman R, Stephany A, Legrand N, Laugier M and Ponthot J-P. MetaLub - a slab method software for the numerical simulation of mixed lubrication regime in cold strip rolling. *Proceedings of the Institution of Mechanical Engineers, Part J: Journal of Engineering Tribology* 2011; 225: 894–904.

[26] Wilson W and Sheu S. Real area of contact and boundary friction in metal forming. *International Journal of Mechanical Science* 1988; 30: 475–489.

[27] Sutcliffe M. Surface asperity deformation in metal forming processes. *International Journal of Mechanical Science* 1988; 30: 847–868.

[28] Jortner D, Osterle D and Zorowski C. An analysis of cold rolling. *International Journal of Mechanical Sciences* 1960; 2: 179–194.

[29] Bair S, Mary C, Bouscharain N and Vergne P. An improved Yasutomi correlation for viscosity at high pressure. *Proceedings of the Institution of Mechanical Engineers, Part J: Journal of Engineering Tribology*, published online on January 28, 2013.

[30] Yasutomi S, Bair S and Winer W. An application of a free-volume model to lubricant rheology (I) Dependence of viscosity on temperature and pressure. *ASME Journal of Tribology* 1984; 106: 291–312.